参赛队员姓名：Amy Jiayin Wang, 陈乐一

中学：上海中学国际部 (SHSID)

省份：上海

国家/地区：中国

指导教师姓名：刘佳龙，曹宵鸣

指导教师单位：上海中学国际部，华东理工大学

论文题目：Methane activation by oxygen species on MN_4 embedded graphene catalyst (M = 3d transition metals): A density functional theory study

Methane activation by oxygen species on MN_4 embedded graphene catalyst (M = period 3d transition metals): A density functional theory study

Authors: Amy Jiayin Wang, 陈乐一

Abstract

The accumulation of methane around the globe would yield much more industrial and economic value if it could be transformed into more valuable products. Under this background, catalysts are needed for these reactions, and single transition atom catalysts have been commonly studied. We use the density functional theory (DFT) computations to compare the adsorption of oxygen on the surface and its activation energies of MN_4 porphyrin-like co-coped graphene systems with different transition metal centers on the methane-to-methanol conversion. The DFT results show that the barriers decrease then increase as the atomic number of 3d transition metal centers increase. Our results show insights about methane activation and subsequent conversion and can lead to further studies for creating efficient graphene-based transition metal catalysts.

Key words

Doped graphene, Density functional theory, Methane activation, Surface reactive oxygen species, Transition metal center

Table of contents

1. Introduction
2. Methodology
3. Results and discussion
    3.1. Oxygen species adsorption
    3.2. Methane Activation
4. Conclusion
5. References

1. Introduction

In recent years, the development of shale gas has promoted a surge in natural gas production. Methane, the primary component of natural gas, has a huge impact on the development of the chemistry industry if converted into more valuable chemicals. The direct conversion of methane (CH_4) to methanol (CH_3OH) is a promising approach to utilize methane because of the high atomic efficiency and low carbon dioxide emission.

However, methane activation remains a major challenge due to the strong C-H bond energy (440 kJ/mol), the low affinity for electrons and protons, low polarizability, and high ionization energy [2]. Furthermore, once the methane is activated, the lower C-H bond of the oxygenates lead to the problem of the catalyst activity being too high, which leads to the deep oxidation of intermediate species into CO_x. Methane activation faces the problem of both difficult activity and high selectivity. Therefore, it draws intensive attentions to find an efficient and economically suitable catalyst that controllably lowers the activation energy and achieves the desired liquid fuels.

Graphene, which has been increasingly studied both experimentally and theoretically in recent years, is known for its special electrical and thermodynamic properties [4]. Doping graphene with metal atoms can further increase its electrical conductive abilities [5], and the excellent thermal conductivity of graphene matrix could efficiently prevent the generation of local hot pot to avoid radical reactions and resulting deep oxidation. Metal-doped graphene's catalytic abilities have been confirmed by experimental studies [6, 7], and heterogeneous atom (such as N) doped graphene also exhibit catalytic behaviors [8, 9]. The type of transition metal that is doped in graphene is one of the many factors that affect the catalytic ability and stability of MN_x-G (metal nitrogen co-doped graphene) [10, 11]. Specifically, MN_4-G has shown to have higher stability than MN_2-G or MN_3-G catalyst [12,13]. Therefore, this work will be investigating MN_4 embedded graphene as the catalyst, with M being 3d transition metals.

Among the possible routes for converting methane, favorable thermodynamics of the oxidation process offers the greatest potential [3]. Different reactive surface oxygen species are generated during the oxidation reaction process, which would trigger a variety of reaction pathways. In general, anion radical $O^{-\cdot}*$ (* denotes the surface intermediates throughout the paper), superoxide $O^{2-\cdot}*$, and peroxide $O_2^{2-}*$ are the surface oxygen species most commonly implicated in methane activation chemistry [14, 15]. A great amount of work has revealed that the H could be abstracted from the methane by $O^{-\cdot}*$, $O^{2-\cdot}*$ or $O_2^{2-}*$ on the catalyst surface [16-19]. One way the different transition metal centered catalyst is investigated is by analyzing the formation of adsorbed surface oxygen species.

This article uses density functional theory (DFT) calculations to investigate the adsorption of oxygen and subsequent activation of methane on MN_4 porphyrin-like co-doped graphene configuration (MN_4-G), which is the first step of methane to methanol conversion. 3d transition metals (M) are examined as the independent variable to explore the trends and differences in adsorption and catalytic properties, thus gain insight into the catalytic oxidation of methane conversion.

2. Methodology

All the calculations were carried out using Vienna Ab-initio Simulation Package (VASP) [20-22] with the projector augmented wave method and cutoff energy of 500 eV. The generalized gradient approximation method was chosen with Perdew-Burke-Ernzerhof (PBE) functional for the exchange-correlation term [23]. The Grimme's empirical three-body dispersion correction in the scheme of Becke-Johnson damping was also included to describe van der Waals interaction.

Periodic slab model was used to simulate the MN_4-graphene catalysts with each cell size of 12.300 Å * 12.783 Å * 15.000 Å. Adsorption geometries underwent optimization using a force-based gradient algorithm until forces for all atoms were below 0.05 eV/Å. The transition states (TSs) of methane activation were searched with a constrained optimization scheme [24]. The optimized state was when the total energy was a maximum in the reaction coordinate, and a minimum compared to the degrees of freedom.

The adsorption energy of the oxygen species on the MN_4-G surface was defined as:

$$E_{ad} = E_x + E_x{*} - E_{sur}$$

where E_{sur} represents the total energy of a co-doped graphene surface, E_x represents the total energy of a gas molecule, and $E_x{*}$ represents the total energy after steady adsorption. Therefore, a more negative value indicates stronger adsorption between the oxygen molecule and MN_4-G system.

3. Results and Discussion

The goal of this work is to investigate the trends and patterns of catalytic activity of different oxygen adsorbed transition metal MN_4-G systems toward methane activation. We computationally compared oxygen adsorption strengths and electronic structure as well as transition state of methane activation from different transition metal systems.

3.1 Oxygen species adsorption

For a catalyst, according to Sabatier's principle, the catalytic performance could be modulated by the adsorption energy of the key adsorbate at the active sites. Finding the most favorable adsorption configurations of O_2 on the studied porphyrin-like co-doped graphene surface is therefore the first step to understanding its catalytic activation abilities. Thus, we investigated the adsorption of O_2 over each transition metal center MN_4-G system (Figure 1). The O_2 molecule accepts electrons in its 2pi orbitals, and adsorbs to the surface.

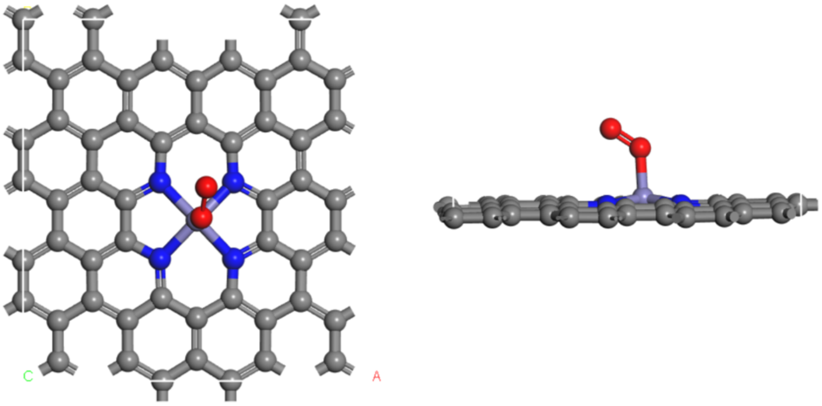

Figure 1. Top and side views of O_2 chemisorption on FeN_4-G at O-end mode.

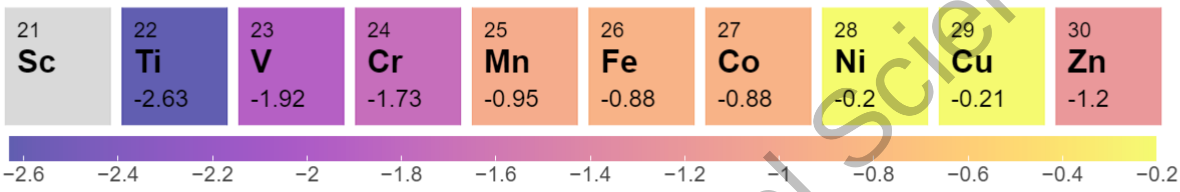

21	22	23	24	25	26	27	28	29	30
Sc	Ti	V	Cr	Mn	Fe	Co	Ni	Cu	Zn
	-2.63	-1.92	-1.73	-0.95	-0.88	-0.88	-0.2	-0.21	-1.2

Figure 2. The adsorption energies (eV) of O_2 on 3d-MN_4-G

The oxygen adsorption strength on MN_4-G from left to right across the periodic table shows a monotonically decreasing tendency until Ni and then slowly increase (Figure 2). The more left-leaning metal atoms have a stronger oxophilicity, the more they are likely to lose electrons to oxygen. It results in the stronger adsorption energy. After Ni, the number of electrons in the d-orbit is saturated, and the increased number of s-orbit electrons causes the enhanced charge transfer and the resulting enhanced adsorption strength.

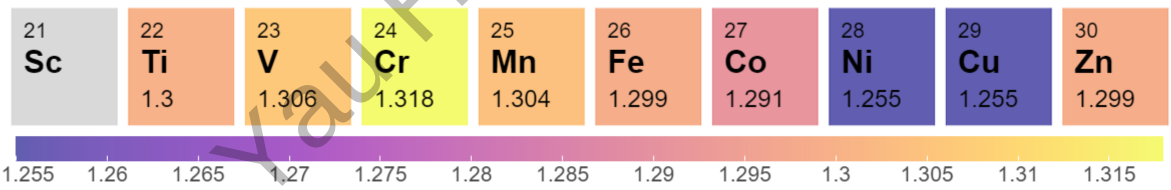

21	22	23	24	25	26	27	28	29	30
Sc	Ti	V	Cr	Mn	Fe	Co	Ni	Cu	Zn
	1.3	1.306	1.318	1.304	1.299	1.291	1.255	1.255	1.299

Figure 3. The O-O bond lengths (Å) of chemisorbed O_2 on 3d-MN_4-G

The oxygen bond length of oxygen at adsorption state (adsorbed onto the central transition metal in the metalloporphyrin structure) can reflect the degree of activation of oxygen molecules. The longer the oxygen bond, the greater effect the metal has on oxygen. The more leftward in the periodic table of elements, the stronger the electron ability of oxygen from the transition metal. Zn's particularity as an example is discussed later.

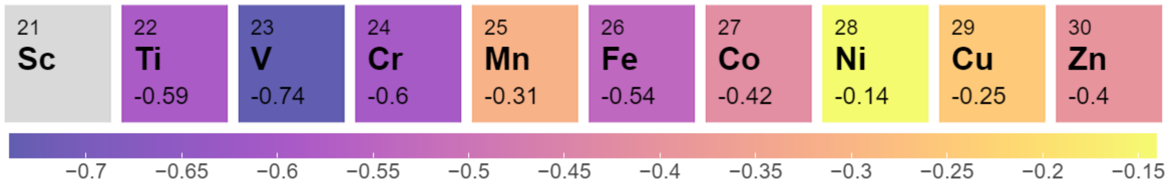

21	22	23	24	25	26	27	28	29	30
Sc	Ti	V	Cr	Mn	Fe	Co	Ni	Cu	Zn
	-0.59	-0.74	-0.6	-0.31	-0.54	-0.42	-0.14	-0.25	-0.4

Figure 4. The Bader charges of the oxygen species on 3d-MN_4-G

The charge of the oxygen over the metalloporphyrin structure from left to right across the periodic table shows a decreasing trend as a whole, which then increases gradually after Ni. The reason for the beginning of the decrease in charge is the reduction of adsorption energy, and the reduction of oxygen from the metal to the electrons. Among them, the charge from Mn to Fe has been almost halved. Mn's five valence electrons occupy five d-orbits, so the sixth electron in Fe has a huge effect on the charge. The metal after Ni is consistent with the result of adsorption energy, because electrons increase in the s orbit, adsorption energy increases with the decrease of electrical negativity, and the charge increases.

3.2 Methane activation

Since the adsorption strength of O_2 is higher than CH_4 [25], when the two reactants are injected to the system, there is a higher likelihood of O_2 occupying the single transition metal atom active site. After adsorption of O_2, which leads to oxygen species occupying the active transition metal site on the MN_4-G surface, oxidative methane activation begins.

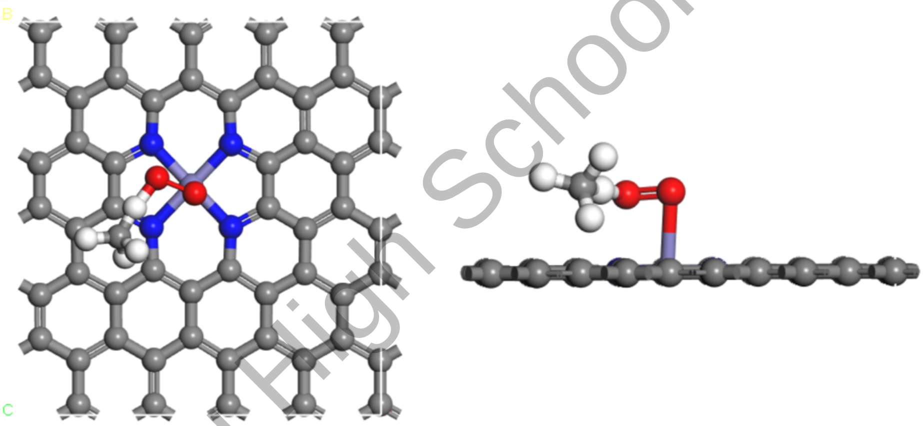

Figure 5. Top and side views of the transition state of methane oxidative dehydrogenation on the FeN_4-G surface

The Eley-Rideal (ER) mechanism has been suggested by previous investigations [26] for the first steps of such oxidation reactions. The mechanism begins with interaction between the gaseous CH_4 and the activated O_2 on a surface (Figure 5). The detailed aspects and calculations of the first step of methane activation on MN_4-G are discussed in the following.

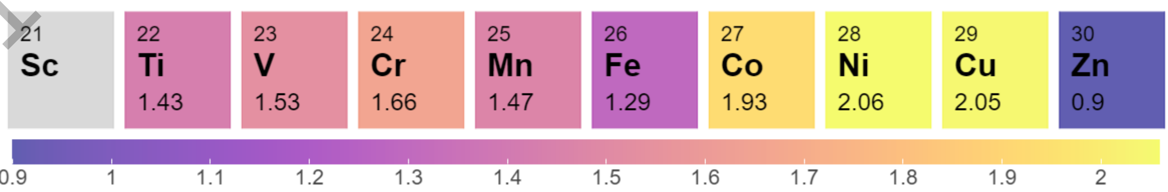

21 Sc	22 Ti	23 V	24 Cr	25 Mn	26 Fe	27 Co	28 Ni	29 Cu	30 Zn
	1.43	1.53	1.66	1.47	1.29	1.93	2.06	2.05	0.9

Figure 6. The energy barriers (eV) of methane oxidative dehydrogenation on 3d-MN_4-G

The activation energy of methane hydrocarbon bonds in the gaseous state is 4.52 eV. All metalloporphyrin oxides activation energy are concentrated in 0.90-2.05 eV, significantly lower than the gaseous activation energy. Metal niche oxides can effectively reduce energy base and increase the likeness of reaction in methane hydrocarbon bond activation reaction. The activation energy of the hydrocarbon bond in methane decreases from left to right on the periodic table of elements to Fe and then rises until Ni.

The activation energy of the hydrocarbon bond in methane decreases from left to right on the periodic table of elements to Fe and then rises until Ni. Atoms' ionization energy increases from left to right on the periodic table. In other words, transition metals with smaller atomic numbers are more likely to contribute electrons with stronger adsorption energy. Oxygen bonds are weakened by strong adsorption, making it easier to activate methane. In the metalloporphyrin oxides after Ni, the electrons of the d-orbit remain unchanged, only the electrons of the s-orbit increase, the electron is negative and decreases, the adsorption is enhanced, and it is not easy to activate methane. So, overall, the more the periodic table leans on the left transition metal-centric zirconium structure activation energy base overall lower, and after Ni rise.

For the leftmost Zn on the periodic table of elements, activation energy suddenly decreases. Chemically, unlike other transition metals in the free d orbit, Zn's 3d orbit is filled, making it difficult for new superoxide to enter or provide new electron structures to adsorb.

Fe exhibits a drop in activation energy, which means that there is less energy needed to reach the transition state. This result correlates with the data of other single transition metal atom activation experiments, in which atomic Fe exhibits a superior intrinsic activity and stability [27].

4. Conclusion

The conversion of methane into methanol with catalysts is a challenge due to methane's properties, but is also very important due to the increased extraction of methane. We explore the adsorption and catalytic ability of oxygen species adsorbed to MN_4-doped graphene with different 3d transition metals, using (density function theory) DFT calculations. The adsorption energy, geometry, charge of adsorbed oxygen molecule, as well as the transition state and activation energy of methane oxidative dehydrogenation are analyzed. We followed the Eley-Rideal reaction mechanism and investigated how different transition metal centers exhibited different catalytic abilities.

Our findings reveal that the most efficient transition metal center, the one showing the lowest activation energy is Fe. The FeM_4-G system has the potential of being an effective catalyst for methane to methanol conversion due to its relative low activation energy and high stability. To the best of our knowledge, this paper conducts a deep investigation on MN_4 porphyrin-like co-doped graphene, a catalyst that has been widely researched, and specifically focusing on how changing the central metal would affect its catalytic ability of activation methane. Our findings may open a new way to design investigations in the next steps of the reaction mechanism.

5. References

[1] M. Bradford, M. Vannice, CO2 reforming of CH4, Catal. Rev. 41 (1999) 1-42.

[2] X. M. Cao, H. Zhou, L. Zhao, X. Chen, P. Hu, et al. Screening performance of methane activation over atomically dispersed metal catalysts on defective boron nitride monolayers: A density functional theory study. Chinese Chemical Letters 32 (6), 1972-1976.

[3] C. Hammond, S. Conrad, I. Hermans, Oxidative methane upgrading, ChemSusChem 5 (2012) 1668-1686.

[4] W. Choi, I. Lahiri, R. Seelaboyina, Y. S. Kang, Synthesis of graphene and its applications: a review, Crit. Rev. Solid State 35 (2010) 52-71.

[5] J. Dai, J. Yuan, Adsorption of molecular oxygen on doped graphene: atomic, electronic, and magnetic properties, Phys. Rev. B 81 (2010) 165414.

[6] A. Krasheninnikov, P. Lehtinen, A. S. Foster, et al., Embedding transition-metal atoms in graphene: structure, bonding, and magnetism, Phy. Rev. Lett. 102 (2009) 126807.

[7] J. A. Rodríguez-Manzo, O. Cretu, F. Banhart, Trapping of metal atoms in vacancies of carbon nanotubes and graphene, ACS Nano 4 (2010) 3422-3428.

[8] Y. Fujimoto, S. Saito, Formation, stabilities, and electronic properties of nitrogen defects in graphene, Phy. Rev. B 84 (2011) 245446.

[9] X. Zhang, Z. Lu, G. Xu, T. Wang, D. Ma, Z. Yang, L. Yang, Single Pt atom stabilized on nitrogen doped graphene: CO oxidation readily occurs via the tri-molecular Eley–Rideal mechanism, Phys. Chem. Chem. Phys. 17 (2015) 20006–20013.

[10] C.W. Bezerra, L. Zhang, K. Lee, H. Liu, A.L. Marques, E.P. Marques, H. Wang, J. Zhang, A review of Fe–N/C and Co–N/C catalysts for the oxygen reduction reaction, Electrochim. Acta 53 (2008) 4937–4951.

[11] J. Luque-Centeno, M. Martínez-Huerta, D. Sebastián, G. Lemes, E. Pastor, M. Lázaro, Bifunctional N-doped graphene Ti and Co nanocomposites for the oxygen reduction and evolution reactions, Renew. Energy 125 (2018) 182–192.

[12] Y. Feng, F. Li, Z. Hu, X. Luo, L. Zhang, X.-F. Zhou, H.-T. Wang, J.-J. Xu, E. Wang, Tuning the catalytic property of nitrogen-doped graphene for cathode oxygen reduction reaction, Phys. Rev. B 85 (2012) 155454.

[13] W. Orellana, Catalytic properties of transition metal–N4 moieties in graphene for the oxygen reduction reaction: evidence of spin-dependent mechanisms, J. Phys. Chem. C 117 (2013) 9812–9818.

[14] M.S. Palmer, M. Neurock, M.M. Olken, J. Am. Chem. Soc. 124 (2002) 8452-8461.

[15] V.J. Ferreira, P. Tavares, J.L. Figueiredo, J.L. Faria, Ind. Eng. Chem. Res. 51 (2012) 10535−10541.

[16] J.H. Lunsford, Catal. Today 6 (1990) 235.

[17] M.Y. Sinev, V.N. Korchak, O. V. Krylov, Kinet. Catal. 27 (1987) 1110-1112.

[18] D. Dissanayake, J.H. Lunsford, M.P. Rosynek. J. Catal. 143 (1993) 286-298.

[19] W. Weng, M. Chen, H. Wan, Y. Liao, Catal Lett. 53 (1998) 42-50.

[20] G. Kresse, J. Furthmuller, Comp. Mater. Sci. 6 (1996) 15-50.

[21] G. Kresse, J. Hafner, Phys. Rev. B 49 (1994) 14251.

[22] G. Kresse, J. Furthmuller, Phys. Rev. B 54 (1996) 11169-11186.

[23] J.P. Perdew, K. Burke, M. Ernzerhof, Phys. Rev. Lett. 77 (1996) 3865-3868.

[24] A. Alavi, P. Hu, T. Deutsch, P.L. Silvestrelli, J. Hutter, Phys. Rev. Lett. 80 (1998) 3650-3653.
[25] P. Nematollahi, E. C. Neyts, Direct methane conversion to methanol on M and MN_4 embedded graphene (M = Ni and Si): A comparative DFT study, Appliced Surface Science 496 (2019) 143618.
[26] G. Xu, R. Wang, F. Yang, D. Ma, Z. Yang, Z. Lu, CO oxidation on single Pd atom embedded defect-graphene via a new termolecular Eley-Rideal mechanism, Carbon 118 (2017) 35–42.
[27] J. Zheng, K. Lebedev, S. Wu, C. Huang, et. al, *Journal of the American Chemical Soceity* 2021 *143* (21), 7979-7990.